Experimental Evaluation and RBFNN Prediction of Mechanical Properties in Madar Fiber–Groundnut Shell Powder Reinforced Epoxy Composites

Ajinkya P Edlabadkar[1], M. Yuvaperiyasamy[2], K.Vinukumar[3], Gokilhashree. M[4]*

[1]Assistant Professor, Department of Mechanical Engineering, Yeshwantrao Chavan College of Engineering, Wanadongri, Nagpur, Maharashtra, India.

[2]Department of Mechanical Engineering, Saveetha School of Engineering, Saveetha Institute of Medical and Technical Sciences (SIMATS), Chennai, Tamil Nadu, India.

[3]Associate Professor, Department of Mechanical Engineering, Francis Xavier Engineering College, Tirunelveli, Tamil Nadu, India.

[4]*Department of Medical Electronics, Sengunthar Engineering College, Thiruchengode, Namakkal, Tamil Nadu, India.

Email ID: [1]ajinkyae@gmail.com, [2]yuvaperiyasamyvsb@gmail.com, [3]dr.vinukumar.k@gmail.com, [4]*murughanandgoki@gmail.com

Abstract

This study investigates the mechanical response of hybrid composites fabricated from Madar fiber, groundnut shell powder, and epoxy resin. The reinforcement and particulate filler were incorporated into the epoxy matrix to develop composites with improved load-bearing characteristics. Mechanical performance was examined through tensile, flexural, impact, and interlaminar shear strength tests, while scanning electron microscopy (SEM) were used to assess fracture morphology and interfacial characteristics. A radial basis function neural network (RBFNN) were additionally developed to estimate tensile and flexural strengths from the material composition. The network employed radial basis neurons to capture nonlinear relationships between the input variables and mechanical responses. Among the investigated compositions, MGE-2 containing 20 wt.% Madar fiber, 15 wt.% groundnut shell powder, and 65 wt.% epoxy resin exhibited the most favorable performance. MGE-2 attained tensile strength of 61.78 MPa and tensile modulus of 3.26 GPa, together with a flexural strength of 94.36 MPa and flexural modulus of 4.78 GPa. Corresponding impact strength and interlaminar shear strength reached 20.68 kJ/m² and 21.37 MPa, respectively. The RBFNN provided reliable predictions, yielding test R^2 values of 0.9204 and 0.9447 for tensile and flexural strengths, respectively.

Keywords: Natural fiber, Mechanical properties, Flexural modulus, Optimization, Artificial Neural Network.

1. Introduction

Composite materials are increasingly used in engineering applications because they offer a favorable combination of low weight, high strength, durability, and design flexibility. The incorporation of natural fibres, agricultural wastes, and functional fillers provides a sustainable route for improving material performance while reducing dependence on conventional synthetic resources. Such composite systems are widely investigated for structural, automotive, construction, packaging, and other lightweight applications. Plantain banana fibre and madar fibre were combined at 40% and 20%, respectively, with 40% epoxy resin to develop a sustainable composite substrate for printed circuit board applications. The hybrid natural-fibre system was designed as an alternative to conventional plastic-based PCB materials (Omprakasam et al., 2025). Peepal, okra, and madar fibres were selected as hybrid natural reinforcements, with 6 wt.% peepal fibre and varying okra/madar contents. TiO_2 nanopowder at 2, 4, 6, and 8 wt.% was additionally introduced to enhance wear resistance and

tribological performance (K et al., 2026). Groundnut shell powder is an agro-waste filler that can be incorporated into epoxy-based natural fibre composites to modify their mechanical and physical characteristics. Its proportion influences interfacial interaction, stiffness, impact response, and the overall microstructure of the composite system (Sathish, 2024).

Glass fibre and madar fibre were hybridized in an epoxy resin matrix and further modified using porcelain particles as an inorganic filler. The material combination was developed to improve structural, viscoelastic, and thermal characteristics of the hybrid composite (Raja et al., 2024). The hybrid composite laminates were fabricated using the hand lay-up technique with 70% epoxy resin and 30% fibre reinforcement. Bamboo, jute, and glass fibre layers were manually arranged in the required stacking sequence and impregnated with epoxy to form the laminate (Parvathamma et al., 2027). Groundnut shell powder is a lightweight agricultural residue that can serve as a sustainable particulate modifier in polymer-based friction materials. Its lignocellulosic nature, low cost, and availability make it suitable for reducing dependence on conventional synthetic fillers in wear-related applications (Gore et al., 2025). Sugarcane bagasse/PLA, rice husk silica/ABS, coir fibre/PHA, bamboo particle/nylon, and groundnut shell powder/PETG were considered. These agricultural-waste-based composites were compared based on technical, environmental, and economic material characteristics (Kathirvel et al., 2026). Groundnut shell powder is an agro-waste filler that can be incorporated into epoxy-based natural fibre composites to modify their mechanical and physical characteristics. Its proportion influences interfacial interaction, stiffness, impact response, and the overall microstructure of the composite system (Sathish, 2024).

Groundnut shell powder was processed to obtain cellulose microfibres and combined with agar to fabricate biodegradable. Three film systems agar, agar/peanut shell powder, and agar/cellulose microfibre were developed for sustainable packaging applications (Kaur et al., 2025). Jute fibres were coated with aloe vera gel and reinforced in an epoxy matrix containing cellulose- and non-cellulose-based fillers. Groundnut shell powder, teakwood powder, and graphene were selected as particulate modifiers to enhance the mechanical behaviour of the composite (Phani Prasanthi et al., 2024). Groundnut shell is an abundant agricultural by-product with a lignocellulosic structure rich in cellulose, hemicellulose, and lignin. Its low density, biodegradability, availability, and surface functional groups make it suitable for use in composites, adsorbents, biochar, and other value-added materials (Jain et al., 2025).

Groundnut shell powder, coconut coir powder, and H_3PO_4-activated corn leaf carbon were employed as low-cost biosorbents for Acid Blue 113 removal. Their adsorption behaviour was compared under varying pH, concentration, temperature, contact time (Sunkar et al., 2023). Groundnut shell ash was incorporated at 2, 4, 6, and 8% into lime-stabilized lateritic soil to improve its engineering performance. The combined lime–GSA system was evaluated as a sustainable stabilizing material (Adetayo et al., 2021). Lateritic soils were modified using optimum lime content together with 2–6% groundnut shell ash as an agricultural-waste-derived stabilizer. The developed soil–lime–GSA mixtures were investigated for potential use in highway structural applications (Amu et al., 2021). Epoxy resin was reinforced with a constant 30 wt.% jute fabric and groundnut shell powder at 0, 5, 10, 15, and 20 wt.%. The agro-waste filler was incorporated to modify the physical, mechanical, and interfacial characteristics of the jute/epoxy composite (Patnaik et al., 2022). Groundnut shell and other agricultural wastes are abundant, renewable, and low-cost biomass resources that can be converted into useful engineering materials. Their lignocellulosic composition and biodegradable nature support applications in composites, construction products, adsorbents, and bio-based fillers, while reducing waste disposal and environmental impact (Nakkeeran et al., 2025). Madar fibre and

sugarcane bagasse ash were incorporated into an epoxy matrix to form hybrid bio-composites using compression moulding. A formulation containing 28 wt.% madar fibre and 7 wt.% bagasse ash was investigated as a sustainable reinforcement–filler system (Chandrika et al., 2022).

The novelty of this study lies in the development of a hybrid epoxy composite combining Madar fiber and groundnut shell powder as sustainable reinforcements, together with the application of a radial basis function neural network (RBFNN) for predicting its mechanical performance. The work integrates experimental mechanical characterization, SEM-based fracture analysis, and nonlinear data-driven prediction to establish composition–property relationships and identify a suitable hybrid formulation for improved structural performance.

2. Materials and methodology

2.1. Materials used

The composite system consisted of Madar fiber, groundnut shell powder (GSP), and epoxy resin. Madar fiber served as the primary fibrous reinforcement, while finely processed groundnut shell powder was incorporated as the particulate reinforcement. Epoxy resin formed the continuous matrix and provided bonding between the reinforcement phases. The selected constituents were combined at different weight fractions to examine the influence of GSP loading on the physical and mechanical characteristics of the composite. The material proportions were selected with the epoxy content beginning at 70 wt.%, while the Madar fiber content was maintained at 20 wt.%.

2.2. Composite Fabrication

The quantities of Madar fiber, groundnut shell powder, and epoxy resin required for each composition were determined on a weight basis. Composite panels were produced through the hand lay-up technique (Vyas & Jhala, 2027). Initially, the mould surface was cleaned and covered with a release film to facilitate removal after curing. The required amount of GSP was dispersed uniformly in the epoxy matrix, followed by the addition of the curing agent. Madar fiber layers were then positioned inside the mould, and the prepared GSP/epoxy mixture was distributed over the reinforcement to achieve adequate impregnation. Successive layers were arranged and compacted to minimize trapped air and obtain uniform panel thickness. A 45 kg compressive load was maintained over the closed mould for 20 h during curing. The cured laminates were subsequently removed and cut according to the dimensions required for individual characterization tests. The processing sequence is presented in Fig. 1.

Table 1. Formulation of Madar fiber/GSP/epoxy composites

Sl. No.	Madar fiber (wt.%)	Groundnut shell powder (wt.%)	Epoxy resin (wt.%)	Composite code
1	20	10	70	MGE-1
2	20	15	65	MGE-2
3	20	20	60	MGE-3
4	20	25	55	MGE-4

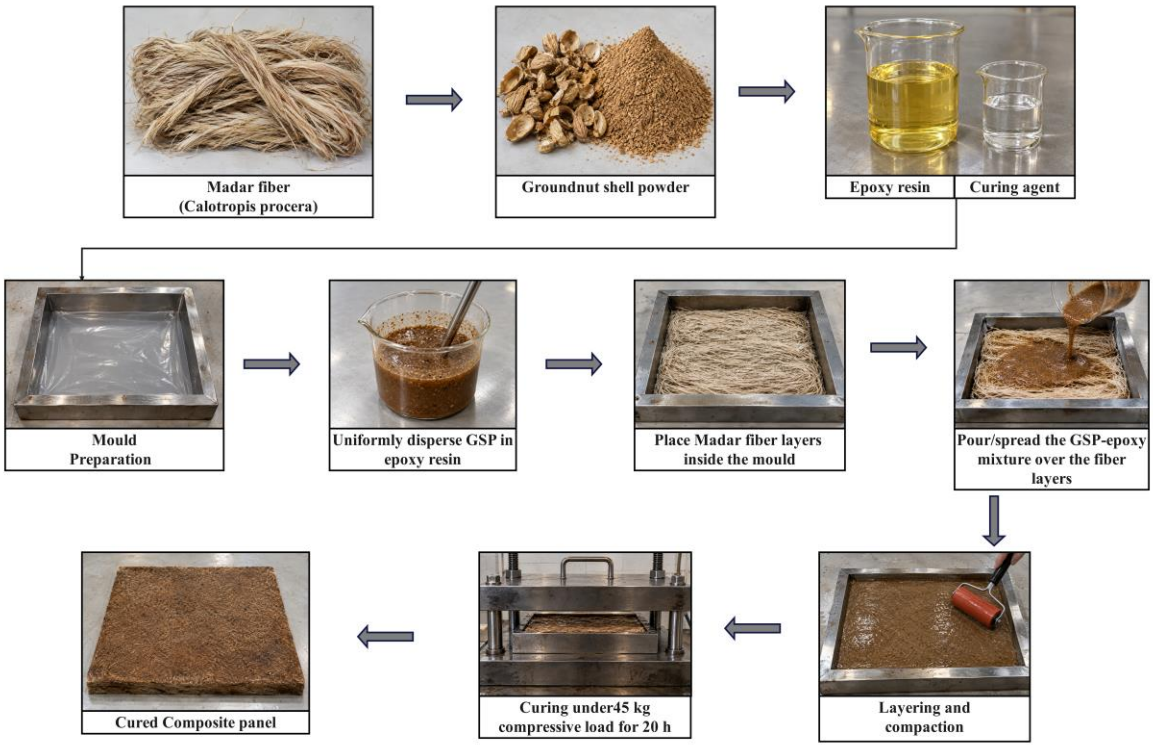

Figure 1. Processing route for Madar fiber/GSP/epoxy composite laminates.

2.3. Constituent Volume Fraction

The volume contribution of each constituent was determined from its weight fraction and density. The composite density and corresponding volume fractions were evaluated using Eqs. (1)-(4).

$$\rho_c = \frac{1}{\left(\frac{W_M}{\rho_M} + \frac{W_G}{\rho_G} + \frac{W_E}{\rho_E}\right)} \tag{1}$$

$$V_M = \frac{W_M \rho_c}{\rho_M} \tag{2}$$

$$V_G = \frac{W_G \rho_c}{\rho_G} \tag{3}$$

$$V_E = \frac{W_E \rho_c}{\rho_E} \tag{4}$$

where ρ_c, ρ_M, ρ_G, and ρ_E denote the densities of the composite, Madar fiber, GSP, and epoxy resin, respectively. V_M, V_G, and V_E represent their corresponding volume fractions.

2.4. Mechanical and Microstructural Characterization

Tensile, flexural, and interlaminar shear strength (ILSS) measurements were carried out using a UTM fitted with 20 kN load cell. Tensile specimens measuring 250 × 25 × 3.3 mm were tested according to ASTM D3039/D3039M at crosshead speed of 2 mm/min (Asif et al., 2026). Three-point bending was performed according to ASTM D790 by specimens of 127 × 12.7 × 3.3 mm at 2 mm/min. ILSS specimens measuring 60 × 12 × 3.2 mm were evaluated

following ASTM D2344/D2344M (Kotik & Perez Ipiña, 2019). Five specimens from each composition were examined, and the mean response and standard deviation were determined.

Impact resistance was measured by the Izod method using specimens of 63.7 × 12.7 × 3.3 mm following ASTM D256 (Grosious & Lakshmaiya, 2026). Rockwell hardness measurements were obtained with a 0.25-inch ball indenter under a 60 kg load in accordance with ASTM D785. Fractured surfaces were subsequently examined using a ZEISS Gemini scanning electron microscope at 20 kV. The micrographs were assessed for fiber pull-out, matrix fracture, particle distribution, interfacial separation, void formation, and crack propagation.

2.5. RBFNN-Based Strength Prediction

A radial basis function neural network (RBFNN) employed to predict tensile and flexural strengths of the Madar fiber/groundnut shell powder/epoxy resin composites (Zhao et al., 2026). The RBFNN was selected because its radial basis neurons can capture nonlinear relationships between composition variables and mechanical responses. The network framework adopted for the prediction process is illustrated in Fig. 2.

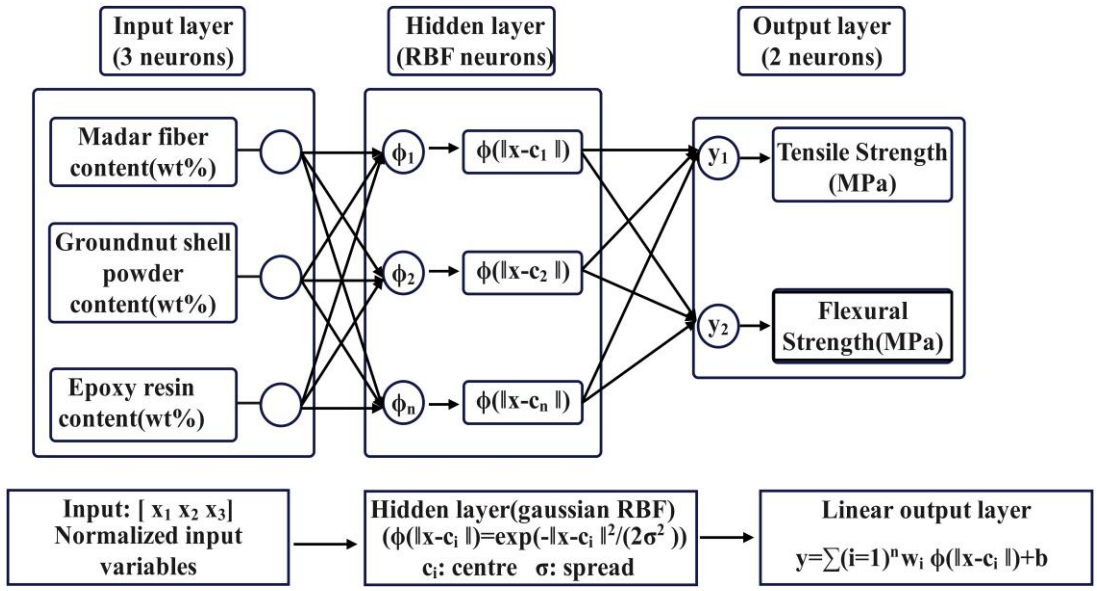

Figure 2. RBFNN framework for predicting mechanical properties of Madar fiber/GSP/epoxy resin composites.

The network received three input variables: Madar fiber content, groundnut shell powder content, and epoxy resin content. Gaussian radial basis functions was employed in hidden layer, while linear transfer function were applied at output layer. Tensile strength and flexural strength were treated as the response variables. Input data were normalized before network training to reduce scale-related effects and improve numerical consistency.

A dataset containing 200 observations was used for network development. The data were randomly divided into 70% for training, 15% for validation, and 15% for testing. Training subset were used to establish relationship between input variables and target responses, whereas the validation subset was employed to select the radial spread and control model generalization. Independent testing subset were retained for final assessment of predictive

capability. Spread parameter was varied systematically, and the value providing the lowest validation error was selected for each response.

Model performance were evaluated by coefficient of determination (R^2), root mean square error (RMSE), and mean absolute error (MAE). R^2 were used to determine the agreement between target and predicted responses, while RMSE and MAE quantified the magnitude of prediction errors. Experimental-versus-predicted plots and residual distributions were subsequently used to examine the predictive behavior of the developed RBFNN.

3. Results and discussion

3.1. Tensile Behaviour of the Composites

The tensile response varied noticeably with groundnut shell powder content, as shown in Fig. 3. Among the four compositions, MGE-2 exhibited the highest tensile strength and modulus, reaching 61.78 MPa and 3.26 GPa, respectively. MGE-1 showed lower values of 54.63 MPa and 2.84 GPa. Increasing the groundnut shell powder content beyond 15 wt.% reduced the tensile performance with MGE-3 recording 57.41 MPa and 3.08 GPa, followed by MGE-4 with the lowest values of 49.86 MPa and 2.71 GPa. Thus, an intermediate filler concentration provided a more favorable tensile response than either lower or higher loading.

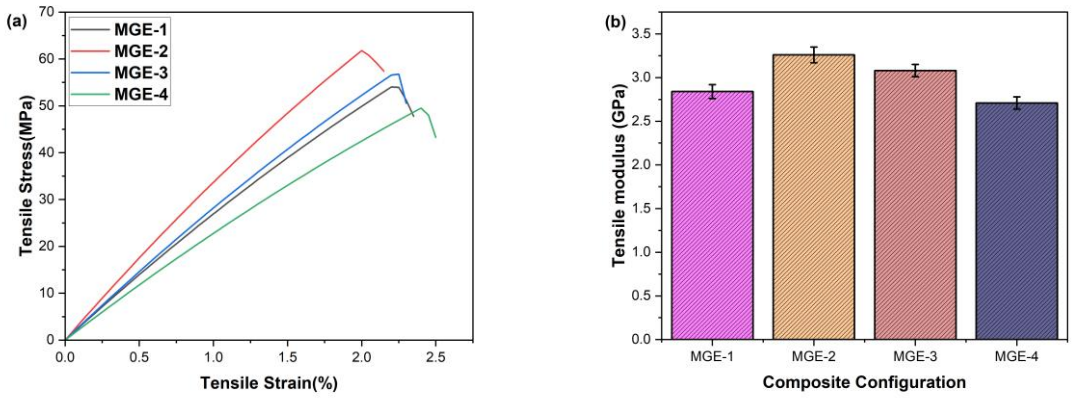

Figure 3. Tensile characteristics of Madar fiber/groundnut shell powder/epoxy resin composites: (a) tensile stress–strain response and (b) tensile modulus.

Relative to MGE-1, MGE-3, and MGE-4, the tensile strength of MGE-2 was higher by approximately 13.09%, 7.61%, and 23.91%, respectively. Its tensile modulus increased by approximately 14.79%, 5.84%, and 20.30%, respectively. The improvement at 15 wt.% groundnut shell powder can be associated with effective reinforcement distribution within the epoxy resin and improved stress transmission between the matrix, particles, and Madar fibers. Under tensile loading, the Madar fibers provide the principal reinforcement, while well-dispersed groundnut shell particles can assist the surrounding matrix in transferring the applied stress.

A further increase in groundnut shell powder caused a progressive decline in tensile properties. At higher particle concentrations, the available epoxy resin decreased from 65 wt.% in MGE-2 to 60 and 55 wt.% in MGE-3 and MGE-4, respectively. This condition can reduce matrix continuity and restrict complete wetting of the reinforcement. Particle-rich regions may also facilitate crack initiation and promote localized stress concentration under tensile loading.

Consequently, the advantages obtained at moderate GSP loading were diminished when its concentration reached 20–25 wt.%.

The tensile modulus followed a similar pattern, confirming the favorable balance between reinforcement and matrix at the MGE-2 composition. Excessive particulate content can also restrict deformation of the epoxy network and reduce the ability of the composite to accommodate tensile strain. Therefore, the 20 wt.% Madar fiber/15 wt.% groundnut shell powder/65 wt.% epoxy resin composition provided the most effective combination for tensile load transfer among the investigated formulations. In previous study, jute/banana fibre–groundnut shell biochar/epoxy composites were evaluated with different stacking sequences and 12–21% biochar. The S2 sequence (J1-B1-J1-B1-J1) achieved the highest tensile strength of 32.58 MPa, owing to improved interfacial bonding and effective load transfer (Yadav & Mishra, 2026).

3.2. Flexural Behaviour of the Composites

The flexural responses of the Madar fiber/groundnut shell powder/epoxy resin composites are presented in Fig. 4. A clear improvement was observed from MGE-1 to MGE-2, with MGE-2 exhibiting the highest FS of 94.36 MPa and FM of 4.78 GPa. MGE-1 recorded 84.52 MPa and 4.16 GPa, respectively. Further addition of groundnut shell powder reduced the bending performance, resulting in flexural strengths of 88.17 MPa for MGE-3 and 76.43 MPa for MGE-4, with corresponding moduli of 4.43 and 3.72 GPa. The steeper response of MGE-2 indicates greater resistance to bending deformation, whereas MGE-4 displayed the lowest flexural stiffness.

Compared with MGE-1, MGE-3, and MGE-4, the flexural strength of MGE-2 was approximately 11.64%, 7.02%, and 23.46% higher, respectively. Its flexural modulus was also greater by 14.90%, 7.90%, and 28.49%, respectively. The improved response at 15 wt.% groundnut shell powder indicates an effective balance between the fibrous reinforcement, particulate phase, and epoxy matrix. During three-point bending, the upper region experiences compression, the lower region undergoes tension, and shear develops through the intermediate region. Therefore, efficient stress transfer among the constituents is essential for maintaining resistance against bending deformation.

The enhanced flexural performance of MGE-2 can be related to the effective contribution of Madar fiber and groundnut shell powder within the epoxy resin. Madar fibers resist tensile stresses developed on the lower side of the specimen, while the epoxy matrix transfers the applied load and maintains structural continuity. At an appropriate concentration, groundnut shell particles can occupy available spaces within the matrix and contribute to resistance against deformation. This combination improves stress distribution and delays the development of bending-induced cracks.

Increasing the groundnut shell powder content beyond 15 wt.% produced the opposite effect. The epoxy resin fraction decreased from 65 wt.% in MGE-2 to 60 wt.% in MGE-3 and 55 wt.% in MGE-4, reducing the amount of matrix available to wet and bind the reinforcement. Higher particle concentration can also increase particle-to-particle interaction and create localized regions susceptible to stress concentration. Under bending, these regions facilitate interfacial separation and crack initiation, thereby reducing both flexural strength and stiffness.

The lowest flexural properties obtained for MGE-4 indicate that excessive groundnut shell powder does not continuously improve bending resistance. Adequate epoxy resin is

necessary to maintain interfacial bonding and transfer stress effectively between the Madar fibers and particulate reinforcement. Accordingly, the 20 wt.% Madar fiber/15 wt.% groundnut shell powder/65 wt.% epoxy resin composition (MGE-2) provided the most favorable flexural response among the investigated composites. In previous work, the madar fibre/bran nanofiller–epoxy composite showed improved flexural performance with increasing madar fibre content. The fibre-rich sample A exhibited the highest flexural strength of 24.14 MPa, indicating more effective reinforcement and load transfer within the matrix (Raja et al., 2023).

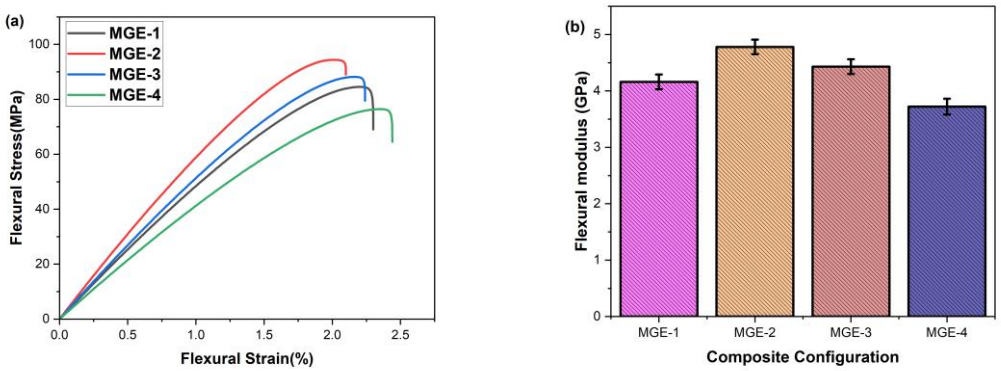

Figure 4. Flexural behaviour of Madar fiber/groundnut shell powder/epoxy resin composites: (a) flexural stress–strain curves and (b) FM.

3.3. Impact Resistance and Energy Absorption

The impact behaviour of the Madar fiber/groundnut shell powder/epoxy resin composites is presented in Fig. 5. The response improved from MGE-1 to MGE-2, whereas further addition of groundnut shell powder caused a gradual decline. MGE-2 exhibited the highest impact strength of 20.68 kJ/m², demonstrating better resistance to sudden loading than the remaining compositions. MGE-1, MGE-3, and MGE-4 recorded lower impact strengths of 18.42, 19.31, and 16.87 kJ/m², respectively. A similar variation was observed for absorbed impact energy, confirming the favorable impact response of MGE-2.

Compared with MGE-1, MGE-3, and MGE-4, the impact strength of MGE-2 was approximately 12.27%, 7.09%, and 22.58% higher, respectively. This improvement can be associated with effective interaction among Madar fiber, groundnut shell powder, and epoxy resin at the intermediate particle concentration. During impact loading, Madar fibers contribute to resistance against rapid fracture, while the surrounding epoxy matrix transfers impact stress across the reinforced region. Groundnut shell particles at an appropriate concentration can further obstruct crack growth and increase the energy required for fracture.

The 15 wt.% groundnut shell powder incorporated in MGE-2 provided a suitable reinforcement level without excessively reducing the epoxy resin fraction. Effective particle distribution can create a more tortuous crack path, requiring additional energy for crack propagation. Madar fibers can also bridge developing cracks and restrict their rapid extension. Together, these mechanisms improve energy dissipation and delay catastrophic failure under impact loading.

At higher groundnut shell powder contents, impact resistance decreased. Increasing the particle fraction to 20 and 25 wt.% simultaneously reduced the epoxy resin content to 60 and 55 wt.%, respectively. The reduced matrix fraction can limit complete reinforcement wetting

and weaken stress transfer between adjacent phases. Higher particle concentrations may also encourage localized particle-rich regions and interfacial discontinuities, which act as preferential sites for crack initiation during sudden loading. These effects explain the lower impact response of MGE-3 and particularly MGE-4.

Overall, the impact results demonstrate that increasing particulate reinforcement beyond an appropriate concentration does not continuously enhance toughness. The 20 wt.% Madar fiber/15 wt.% groundnut shell powder/65 wt.% epoxy resin composition (MGE-2) provided the most favorable balance of fiber reinforcement, particulate content, and matrix continuity for resisting impact-induced fracture. In earlier work, Linear low-density polyethylene (LLDPE) was reinforced with 20 wt.% basalt fibre and alkali-treated groundnut shell powder (T-GSP) at 0, 5, 10, and 15 wt.%. The composite containing 15 wt.% T-GSP + 20 wt.% basalt fibre showed the best overall mechanical performance. However, its impact strength decreased by 14.32% compared with neat LLDPE, indicating that the increased stiffness and filler loading reduced impact resistance (P. Kumar et al., 2023).

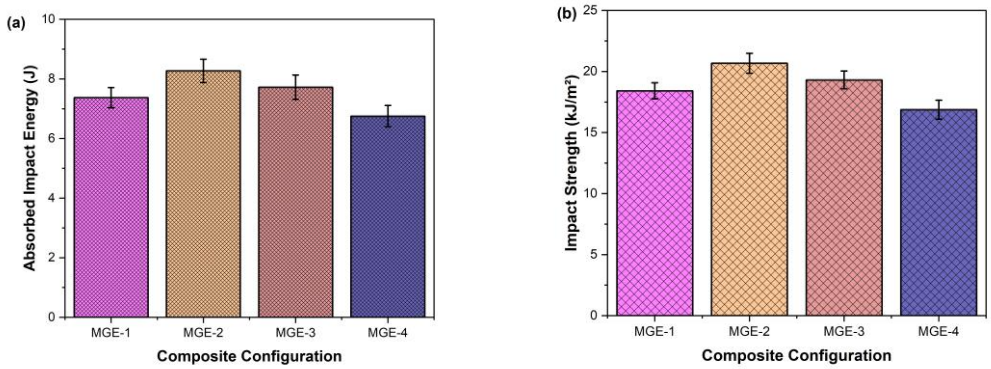

Figure 5. Impact performance of Madar fiber/groundnut shell powder/epoxy resin composites: (a) absorbed impact energy and (b) impact strength.

3.4. Interlaminar Shear Behaviour

The load–displacement response and interlaminar shear strength (ILSS) of the Madar fiber/groundnut shell powder/epoxy resin composites are presented in Fig. 6. Among the investigated compositions, MGE-2 exhibited the highest ILSS of 21.37 MPa, indicating greater resistance to interfacial shear failure. MGE-1, MGE-3, and MGE-4 recorded ILSS values of 18.64, 19.52, and 16.73 MPa, respectively. The maximum load followed a comparable trend with MGE-2 sustaining the greatest load before interlaminar failure.

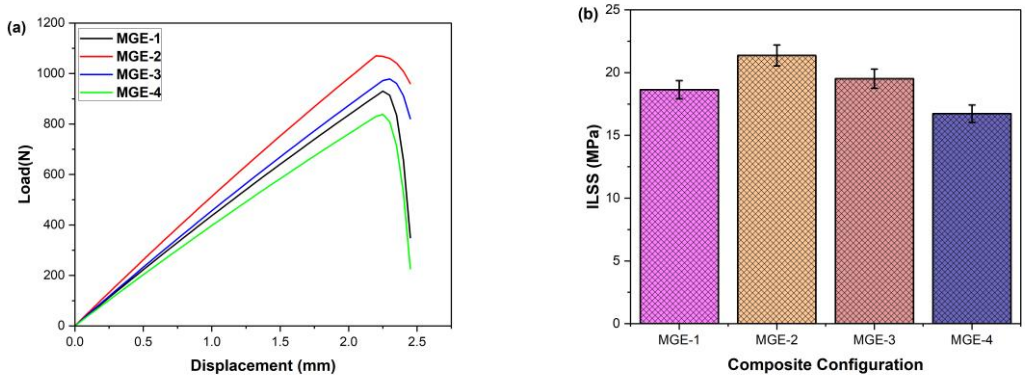

Figure 6. Interlaminar shear response of Madar fiber/groundnut shell powder/epoxy resin composites: (a) load–displacement curves and (b) interlaminar shear strength.

The ILSS of MGE-2 was approximately 14.65%, 9.48%, and 27.74% higher than that of MGE-1, MGE-3, and MGE-4, respectively. The improvement at 15 wt.% groundnut shell powder indicates more effective stress transmission across the reinforcement–matrix interfaces. Adequate epoxy resin surrounding the Madar fibers and GSP helps maintain interfacial continuity, allowing shear stresses to be transferred through the composite without premature separation.

Madar fibers contribute to structural stability by carrying the applied load, while the epoxy resin maintains bonding between adjacent reinforcement regions. At the MGE-2 composition, groundnut shell particles can occupy spaces within the matrix and assist in distributing localized stresses. This arrangement restricts interfacial crack development and delays delamination, thereby improving both the maximum supported load and ILSS.

Further increasing the groundnut shell powder content reduced the interlaminar shear performance. In MGE-3 and MGE-4, the epoxy resin fraction decreased to 60 and 55 wt.%, respectively. A lower matrix fraction can reduce reinforcement wetting and produce weak interfacial regions. Higher particle concentrations can additionally create localized stress concentration, facilitating interfacial separation when subjected to shear loading. These effects were more pronounced in MGE-4, which exhibited the lowest ILSS.

The results indicate that interfacial bonding is a major factor governing the shear resistance of the composite. The 20 wt.% Madar fiber/15 wt.% groundnut shell powder/65 wt.% epoxy resin composition (MGE-2) provided the most favorable reinforcement–matrix interaction and consequently exhibited the highest resistance to interlaminar failure. In earlier research, the hybrid composite containing 30 vol.% fibre (1:1 luffa fibre shell fibre) and 10 vol.% Al_2O_3 exhibited the highest shear strength, indicating improved interfacial bonding between the fibres, alumina filler, and epoxy matrix (Senthil Kumar et al., 2024).

3.5. Rockwell Hardness Behaviour

The Rockwell hardness response of the Madar fiber/groundnut shell powder/epoxy resin composites is presented in Fig. 7. A noticeable variation in indentation resistance was observed with changes in groundnut shell powder content. Among the investigated compositions, MGE-2 exhibited the highest Rockwell hardness value of 92.4, followed by MGE-3, MGE-1, and MGE-4 with values of 88.1, 84.7, and 79.6, respectively. The improved

hardness of MGE-2 indicates that the selected reinforcement ratio provided greater resistance to localized surface deformation.

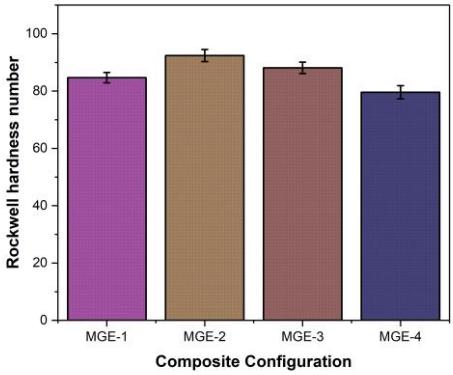

Figure 7. Rockwell hardness of Madar fiber/groundnut shell powder/epoxy resin composites.

Compared with MGE-1, MGE-3, and MGE-4, the hardness of MGE-2 was approximately 9.09%, 4.88%, and 16.08% higher, respectively. The improvement can be associated with effective interaction between Madar fiber, groundnut shell particles, and the epoxy matrix. At 15 wt.% GSP, the particles can occupy available regions within the matrix and restrict localized deformation, while the Madar fibers contribute rigidity and support the surrounding matrix under indentation loading.

The decrease in hardness at higher GSP concentrations indicates that increasing particle content beyond an appropriate level adversely affects surface resistance. For MGE-3 and MGE-4, the reduction in epoxy resin content limits the matrix available for complete reinforcement wetting and bonding. Higher particle concentrations can also produce particle-rich regions and interfacial discontinuities, reducing the uniform transmission of indentation loads. These effects become more pronounced in MGE-4, resulting in the lowest hardness among the investigated compositions.

The relatively lower value of MGE-1 indicates that insufficient GSP content provides less resistance to localized matrix deformation. Therefore, hardness does not increase continuously with either matrix or particulate content; instead, it depends on an appropriate balance among all three constituents. The 20 wt.% Madar fiber/15 wt.% groundnut shell powder/65 wt.% epoxy resin composition (MGE-2) provided the most favorable resistance to indentation. In previous investigation, Peepal, okra, and madar fibres were used as hybrid natural reinforcements, with 6 wt.% Peepal fibre and varying okra/madar fibre contents, while TiO_2 nanopowder at 2, 4, 6, and 8 wt.% was incorporated as a filler. The filler-free composite containing 15 wt.% okra and 15 wt.% madar fibres showed the best overall mechanical performance, whereas 6 wt.% TiO_2 produced the lowest wear rate (K et al., 2026).

3.6. SEM Examination of Fractured Surfaces

The fracture morphologies of composites of Madar fiber/groundnut shell powder/epoxy resin are shown in Fig. 8. The MGE-1 fracture surface in Fig. 8(a) contains clear evidence of fiber pull-out and matrix debris, which means that there may have been poor stress transfer at some fiber–matrix interfaces. The epoxy matrix is surrounding the reinforcement, but there are some areas of debonding and large volume of detached matrix fragments, showing that the lower groundnut shell powder content gives only partial resistance to crack propagation.

The fracture surface shown in Figure 8(b) of the MGE-2 is more compact and shows a scattering of particles with only isolated voids. The particles of the groundnut shell are evenly spread in the epoxy matrix and the concentration of the particles is not too high, which means that the interaction between the particulate phase, Madar fibers, and matrix is improved. The lower fiber pullout and interfacial separation is consistent with the higher tensile, flexural, impact, ILSS and hardness results measured for MGE-2.

A surface similar to that of MGE-3 (Fig. 8(c)) has rough fibers and matrix cracks. The roughened surface of the reinforcement implies mechanical interlock with the surrounding epoxy with the visible matrix crack indicating localized stress concentrations built up during loading. The increased amount of GSP and lower epoxy fraction may make it harder to wet-out the reinforcement fully and therefore more likely to initiate cracks and less efficient to transfer the stress to the reinforcement than MGE-2.

It is observed from Fig. 8(d) that significant number of particles are agglomerated along the fractured region for MGE-4. GSP particles form non-uniform particulate distribution and weak zones in the matrix. If the epoxy content is lowered, say to 25 wt. % GSP, it is not enough to fully encapsulate all of the particles and there will be a tendency to cluster together and form discontinuities at the particle-epoxy interface. The lower mechanical performance of MGE-4 can be attributed to these agglomerated areas that may be preferential crack initiation and propagation sites.

The SEM observation shows that the fracture morphology of MGE-2 with the composition of 20 wt.% Madar fiber, 15 wt.% groundnut shell powder and 65 wt.% epoxy resin is the most favorable. The fracture morphology of other samples is less desirable due to comparatively large variation in particle distribution and the presence of a large number of severe interfacial defects. Fiber pull-out, matrix cracking, void formation and particle agglomeration, become more apparent in the other compositions, especially at higher loading of GSP. In earlier work, Sisal fibre and groundnut shell powder were reinforced. The 20:80 composite showed the highest tensile strength, 100:0 gave the best flexural and impact strength, and 60:40 exhibited maximum hardness. SEM revealed differences in fibre–matrix bonding, fibre pull-out, cracks, and fracture morphology (K. S. Kumar et al., 2025).

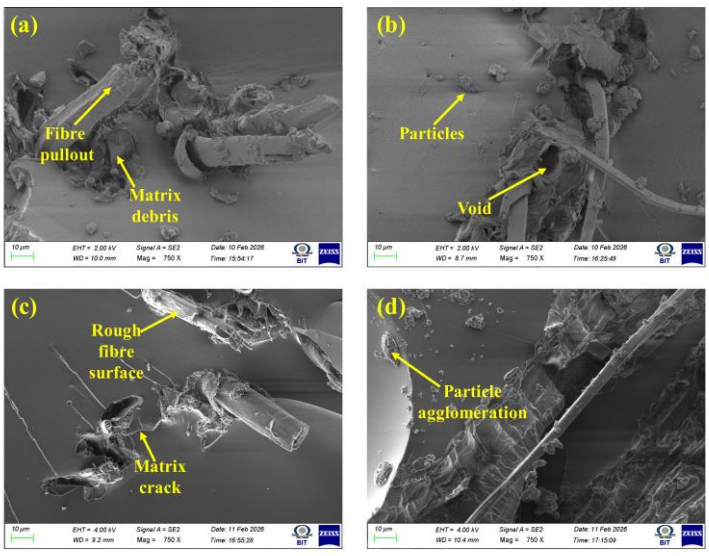

Figure 8. SEM fracture morphologies of Madar fiber/groundnut shell powder/epoxy resin composites: (a) MGE-1, (b) MGE-2, (c) MGE-3, and (d) MGE-4.

3.7. RBFNN Prediction Performance

Predictive performance of radial basis function neural network (RBFNN) for the mechanical responses is presented in Fig. 9. The parity plots show close agreement between the target and RBFNN-predicted values. For tensile strength, model achieved R^2 values of 0.9678, 0.8916, and 0.9204 for the training, validation, and testing subsets. Corresponding values for flexural strength were 0.9650, 0.9547, and 0.9447. These results demonstrate that, the RBFNN effectively captured the nonlinear relationship between Madar fiber, groundnut shell powder, epoxy resin content, and the resulting strength characteristics.

For the testing subset, tensile strength produced an RMSE of 1.5666 MPa and MAE of 1.2989 MPa, whereas flexural strength yielded an RMSE of 2.0360 MPa and MAE of 1.6648 MPa. The relatively small prediction errors and clustering of the data around 1:1 reference line indicate good agreement of target and predicted responses. Flexural-strength model exhibited a slightly higher testing R^2 than the tensile-strength model, indicating that the RBFNN captured the variation in flexural response particularly well.

Residual analysis further supports the prediction performance. Tensile and flexural residuals were distributed on both sides of the zero-error line without a continuous increasing or decreasing pattern over the predicted response range. The comparison of individual test observations also showed that the RBFNN closely followed variations in both mechanical responses. Overall, the obtained statistical measures demonstrate the capability of the developed RBFNN to predict tensile and flexural strengths within the investigated composition range.

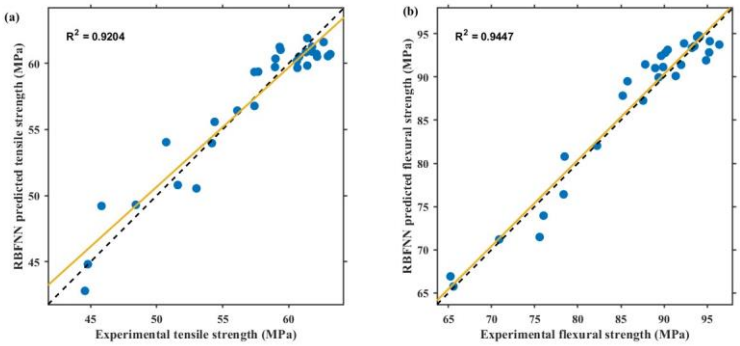

Figure 9. Comparison of target and RBFNN-predicted mechanical responses: (a) tensile strength and (b) flexural strength.

3.8. Potential Engineering Applications

The mechanical characteristics obtained for the Madar fiber/groundnut shell powder/epoxy resin composites indicate potential for lightweight components where moderate structural strength, bending resistance, impact tolerance, and surface hardness are required. Among the investigated formulations, MGE-2, containing 20 wt.% Madar fiber, 15 wt.% groundnut shell powder, and 65 wt.% epoxy resin, provided the most favorable overall mechanical response. Its TS of 61.78 MPa, FS of 94.36 MPa, impact strength of 20.68 kJ/m², and improved interlaminar shear resistance demonstrate its ability to withstand different loading conditions.

The combined fibrous and particulate reinforcement may therefore be considered for lightweight covers, interior automotive panels, furniture components, partition boards, equipment housings, and other semi-structural composite products. The utilization of Madar fiber and groundnut shell powder also provides an opportunity to incorporate plant-derived reinforcement and agricultural residue into epoxy-based composite products. However, application-specific durability, moisture resistance, thermal stability, fatigue behaviour, and long-term performance should be established before employing these composites in demanding service environments.

4. Conclusion

This study evaluated the mechanical performance of Madar fiber/groundnut shell powder/epoxy resin composites through tensile, flexural, impact, interlaminar shear, hardness, and microstructural examinations. The influence of groundnut shell powder content was investigated while maintaining Madar fiber at 20 wt.%, and the major findings are summarized below,

- Among the investigated compositions, MGE-2 containing 20 wt.% Madar fiber, 15 wt.% groundnut shell powder, and 65 wt.% epoxy resin delivered the most favorable overall performance. It attained tensile strength of 61.78 MPa and tensile modulus of 3.26 GPa.

- MGE-2 also achieved high flexural strength and modulus of 94.36 MPa and 4.78 GPa, respectively. Increasing groundnut shell powder beyond 15 wt.% reduced bending performance because the lower epoxy content adversely affected reinforcement–matrix interaction.

- The highest impact strength of 20.68 kJ/m² and ILSS of 21.37 MPa were obtained for MGE-2. Its Rockwell hardness reached 92.4, confirming improved resistance to impact, interlaminar failure, and localized indentation.

- SEM examination of MGE-2 revealed comparatively uniform particle distribution, improved interfacial contact, and fewer prominent defects. Higher groundnut shell powder concentrations increased particle-rich regions, interfacial separation, and void formation, supporting the reduction in mechanical properties.

- The RBFNN effectively predicted the mechanical responses. Testing R^2 values of 0.9204 and 0.9447 were obtained for tensile and flexural strengths, respectively, with RMSE values of 1.5666 and 2.0360 MPa. The results demonstrate the capability of the model within the investigated composition range.

Overall, the Madar fiber/groundnut shell powder/epoxy resin composite shows potential for lightweight and semi-structural components. Further investigation of water absorption, thermal stability, fatigue behaviour, and long-term durability would help establish its suitability for broader engineering applications.

References

Adetayo, O. A., Amu, O. O., Faluyi, F., & Akinyele, E. (2021). Effect of Groundnut Shell Ash on Laterite Soils Stabilized with Lime for Civil Structures. *International Journal of Integrated Engineering*, *13*(4), 242–253. https://doi.org/10.30880/ijie.2021.13.04.023

Amu, O., Adetayo, O., Faluyi, F., & Akinyele, E. (2021). Experimental study of improving the properties of lime-stabilized structural lateritic soil for highway structural works using groundnut shell ash. *Walailak Journal of Science and Technology*, *18*(9). https://doi.org/10.48048/wjst.2021.9475

Asif, L., Hussain, A., Khan, S. A., Baig, M. A. A. S., Shaikh, H. A., Ahmed, W., Najib, A., Loya, A., & Malik, A. N. (2026). Enhancing the Mechanical Performance of Recycled Polyolefins Through Stainless Steel Mesh Reinforcement Processed by Injection Molding. *Journal of Applied Polymer Science*, *143*(40). https://doi.org/10.1002/app.71291

Chandrika, V. S., Anamika, A., Jeeva, C., Perumal, B., Kumar, S. S., Roseline, J. F., & Raghavan, I. K. (2022). Natural Fiber Incorporated Polymer Matrix Composites for Electronic Circuit Board Applications. *Advances in Materials Science and Engineering*, *2022*. https://doi.org/10.1155/2022/3035169

Gore, M., Bhosale, A., Naidu, M., Čep, R., Salunkhe, S., & Nasr, E. A. (2025). Experimental study on polymer friction composite with natural friction modifiers for brake pads. *PLOS ONE*, *20*(9 September). https://doi.org/10.1371/journal.pone.0328987

Grosious, R. E., & Lakshmaiya, N. (2026). Optimization of material extrusion parameters for Izod impact and compressive strength of polycarbonate-graphene composite using Taguchi method and ANOVA. *Hybrid Advances*, *15*. https://doi.org/10.1016/j.hybadv.2026.100743

Jain, S. N., Bhandari, P. S., Bodkhe, M., Chavan, G., Korade, O., Parmar, M., Daware, G. B., & Gautam, N. B. (2025). Adsorptive separation of Acid Red 33 by groundnut shell–based activated carbon. *Biomass Conversion and Biorefinery*, *15*(10), 16003–16013. https://doi.org/10.1007/s13399-024-06424-1

K, A., P, K., M K, M., K, S. M., Kandasamy, K., PVRD, P. R., & B, N. (2026). Enhanced mechanical and tribological properties of Peepal–Okra–Madar fiber hybrid composites reinforced with TiO_2 nanoparticles. *Interactions*, *247*(1). https://doi.org/10.1007/s10751-026-02500-2

Kathirvel, A., Rajendra Thilahar, C., & Gobinath, V. M. (2026). A Linguistic Neutrosophic TOPSIS Framework for Sustainable Biomass Composite Selection. *Neutrosophic Sets and Systems*, *100*, 186–210. https://doi.org/10.5281/zenodo.21957437

Kaur, S., Sidhu, G. K., & Kaur, G. (2025). Development and comparative study of biodegradable packaging film from groundnut shell powder. *Biomass Conversion and Biorefinery*, *15*(22), 29461–29473. https://doi.org/10.1007/s13399-025-06831-y

Kotik, H. G., & Perez Ipiña, J. E. (2019). Suggested modifications of the ASTM D2344-16 short-beam shear test method to be applied to fiber metal laminates. *Journal of Testing and Evaluation*, *49*(2). https://doi.org/10.1520/JTE20170399

Kumar, K. S., Srinivasan, R. G., Palani, S., Čep, R., Salunkhe, S., & Nasr, E. A. (2025). Mechanical characterization of sisal fiber-groundnut shell powder reinforced epoxy composites. *Scientific Reports*, *15*(1). https://doi.org/10.1038/s41598-025-18645-z

Kumar, P., Maiti, T. K., Maurya, A. K., & Adwani, P. (2023). Effect of alkali treated groundnut shell powder in the basalt fiber reinforced polyethylene hybrid composites: A sustainable approach towards green composites. *Polymer Composites*, *44*(7), 3952–3963. https://doi.org/10.1002/pc.27368

Nakkeeran, G., Krishnaraj, L., Alaneme, G. U., & Lawan, M. M. (2025). Mechanical and thermal performance of bio-brick masonry with hydrated lime mortar at high temperature. *Scientific Reports*, *15*(1). https://doi.org/10.1038/s41598-025-06754-8

Omprakasam, S., Vishnu, P., Ishanna, B. M., Abinaya Sree, S., & Divya Rani, R. (2025). Banana fiber with madar fiber composites for sustainable printed circuit boards. *Materials Letters*, *380*. https://doi.org/10.1016/j.matlet.2024.137750

Parvathamma, P. K. S., Kumshikar, R. R., Adeppa, A., Muniswamy, T. K., & Gurbasappa, S. S. (2027). Experimental Study of Woven Glass, Bamboo, and Jute Fibre Reinforced in Epoxy Composites. *Mechanics of Advanced Composite Structures*, *14*(1), 41–56. https://doi.org/10.22075/MACS.2025.37201.1821

Patnaik, P. K., Mishra, S. K., Swain, P. T. R., & Panda, D. (2022). Effect of Groundnut Shell Particulate Content on Physical and Mechanical Behavior of Jute–Epoxy Hybrid Composite. *Journal of The Institution of Engineers (India): Series E*, *103*(1), 65–72. https://doi.org/10.1007/s40034-020-00185-y

Phani Prasanthi, P., Raghavender, V., Venu Madhav, V. V, Sonia, P., Sri Chaitanya, C., Bandhu, D., Saxena, A., & Abdullaev, S. S. (2024). Experimental and simulation study for mechanical properties characterisation of green natural reinforced composites. *International Journal on Interactive Design and Manufacturing*, *18*(5), 3459–3471. https://doi.org/10.1007/s12008-023-01695-w

Raja, T., Devarajan, Y., & Thanappan, S. (2023). Studies on the mechanical and thermal stability of Calotropis gigantea fibre-reinforced bran nano particulates epoxy composite. *Scientific Reports*, *13*(1). https://doi.org/10.1038/s41598-023-42316-6

Raja, T., Yuvarajan, D., Ali, S., Dhanraj, G., & Kaliappan, N. (2024). Fabrication of glass/madar fibers reinforced hybrid epoxy composite: a comprehensive study on the material stability. *Scientific Reports*, *14*(1). https://doi.org/10.1038/s41598-024-53178-x

Sathish, T. (2024). A Comprehensive Analysis of the Physical and Mechanical Responses of Sisal-Epoxy Hybrid Composites to Varied Groundnut Shell Particulate Levels. *Journal of Environmental Nanotechnology*, *13*(2), 5–12. https://doi.org/10.13074/jent.2024.06.242555

Senthil Kumar, M. S., Sivakumar, M., Senthil, S. M., & Rajeshkumar, L. (2024). Effect of alumina fillers on physical and mechanical properties of luffa/groundnut shell natural fiber

reinforced polymer composites. *Polymer Composites*, *45*(11), 10457–10469. https://doi.org/10.1002/pc.28487

Sunkar, S., Prakash, P., Dhandapani, B., Baigenzhenov, O., Kumar, J. A., Nachiyaar, V., Zolfaghari, S., & Hosseini-Bandegharaei, A. (2023). Adsorptive removal of acid blue dye 113 using three agricultural waste biomasses: The possibility of valorization by activation and carbonization – A comparative analysis. *Environmental Research*, *233*. https://doi.org/10.1016/j.envres.2023.116486

Vyas, C. J., & Jhala, R. L. (2027). Experimental Evaluation of Low-Velocity Impact Performance of Glass–Basalt Hybrid Composites: Influence of Fiber Weight Fraction and Impact Energy Levels. *Mechanics of Advanced Composite Structures*, *14*(1), 267–282. https://doi.org/10.22075/macs.2026.37252.1827

Yadav, A. K., & Mishra, S. (2026). Fabrication and characterization of mechanical properties of stacked hybrid composites reinforced with natural fibers and groundnut shell powder as biochar. *Polymers from Renewable Resources*. https://doi.org/10.1177/20412479261461266

Zhao, W., Yang, S., Wu, H., & Dai, J. (2026). Application of the GWO-RBFNN algorithm for data fitting in a sapphire fiber temperature measurement system. *Infrared Physics and Technology*, *154*. https://doi.org/10.1016/j.infrared.2026.106373